Available online at www.sciencedirect.com

Journal of Solid State Chemistry 178 (2005) 2613–2619

JOURNAL OF SOLID STATE CHEMISTRY

www.elsevier.com/locate/jssc

Syntheses and characterization of two new zinc phosphites with 1D chains decorated by Zn-centered complexes

You-Ju Zhong[a], Yong-Mei Chen[b], Yan-Qiong Sun[a], Guo-Yu Yang[a,*]

[a]*State Key Laboratory of Structural Chemistry, Fujian Institute of Research on the Structure of Matter, Chinese Academy of Sciences, Fuzhou, Fujian 350002, China*

[b]*Department of Applied Chemistry, Faculty of Science, Beijing University of Chemical Technology, Beijing 100029, China*

Received 26 March 2005; received in revised form 11 May 2005; accepted 20 May 2005
Available online 7 July 2005

Abstract

Two inorganic–organic hybrid solids, $Zn_2(phen)(HPO_3)_2$ (**1**) and $Zn(phen)(HPO_3)$ (**2**), have been synthesized under solvothermal conditions in the presence of 1,10-phenanthroline (phen) ligands. Their structures were determined by single-crystal X-ray diffraction and further characterized by FTIR, elemental analysis, powder X-ray diffraction, thermogravimetric analysis and fluorescent spectra. Compound **1** crystallizes in the triclnic system, space group P-1, $a = 8.1813(3)$ Å, $b = 8.5535(3)$ Å, $c = 12.3031(5)$ Å, $\alpha = 75.609(1)^\circ$, $\beta = 79.145(2)^\circ$, $\gamma = 67.157(2)^\circ$, $V = 764.46(5)$ Å^3, $Z = 2$. Compound **2** is monoclinic, $C2/c$, $a = 16.1044(7)$ Å, $b = 18.9447(6)$ Å, $c = 8.1713(6)$ Å, $\beta = 94.175(4)^\circ$, $V = 2486.4(2)$ Å^3, $Z = 8$. Both structures consist of 1D chains constructed from strictly alternating ZnO_4 and HPO_3 polyhedra through sharing vertices. The chains are further decorated by Zn-centered complex architectures, $[Zn(phen)]^{2+}$ for **1** and $[Zn(phen)_2]^{2+}$ for **2**. The 2D and 3D supramolecular arrays for **1** and **2** are stably stacked via strong π–π interactions of the phen groups, respectively.

Keywords: Crystal structure; Zinc phosphite; 1,10-phenanthroline; Hydrothermal synthesis

1. Introduction

The search for new open-framework materials has been of great interest in the past few years because of their potential applications in ion-exchange, catalysis, separation processes, etc. [1–3] Since aluminophosphate molecular sieve was synthesized in 1982 [4], a large number of metal phosphates have been prepared in the presence of organic templates to control the shapes and sizes of the channels [3,5]. Recently, the replacement of a tetrahedral phosphate group by a pyramidal phosphite unit has resulted in the preparation of a new class of compounds with various structures, such as clusters [6], chains or ladders [7], layers [8] and 3D frameworks [9].

In some phosphites, templates have also acted as ligands to the metal center [6a,7b,10], featuring a direct Me–N bond between metals and the template molecules. Recently, α- and β-$ZnHPO_3 \cdot N_4C_2H_4$, which feature a direct Zn–N bond between zinc and the template, was reported by Harrison as the first organically templated zinc phosphites [10a]; $(C_5H_6N_2)Zn(HPO_3)$ [10b] and (4,4′-bipy)$[Zn(HPO_3)]_2$ [9j] both contain left- and right-handed helical chains in a sheet; $(NC_5H_{12})_2 \cdot Zn_3(HPO_3)_4$ [9d] has 16-membered ring (MR) windows and $[H_2N(CH_2)_2NH_2]_{0.5} \cdot ZnHPO_3$ possesses an unprecedented architecture of two independent, interpenetrating mixed inorganic–organic networks [7b]. So the syntheses of these materials might potentially lead to a new class of compounds with interesting architectures.

The aim of our work is to pursue new inorganic–organic hybrid luminescent materials using the rigid ligands (2,2′-bipy, 4,4′-bipy and phen) in combination

---

*Corresponding author. Fax: +86 591 83710051.
E-mail address: ygy@fjirsm.ac.cn (G.-Y. Yang).

0022-4596/$ - see front matter © 2005 Elsevier Inc. All rights reserved.
doi:10.1016/j.jssc.2005.05.028

with the d^{10} metals (Zn and Cd). We have now isolated several new phases with hybrid frameworks and luminescent emission [6b,9i,11]. In this paper, we report the syntheses, crystal structures, some properties of two new inorganic–organic hybrid zinc phosphites grafted with phen ligands, $Zn_2(phen)(HPO_3)_2$ (**1**) and Zn(phen) (HPO_3) (**2**). To our knowledge, hybrid solids of **1** and **2** are firstly synthesized in the zinc-phosphite–phen system.

2. Experimental

2.1. Materials and methods

Reagents were purchased commercially and used without further purification. Elemental analyses (C, H, and N) were carried out on an Elementar Vario EL III analyzer. IR spectra were recorded on ABB Bomen MB 102 spectrometer in the 400–4000 cm^{-1} region with pressed KBr pellet. Powder X-ray diffraction (XRD) data were obtained using a Philips X'Pert-MPD diffractometer with Cu-$K\alpha_1$ radiation ($\lambda = 1.54056$ Å). The thermogravimetric analysis was performed on a Netzsch STA 449c analyzer in air atmosphere with a heating rate of 15 °C min^{-1}. Fluorescent spectra were measured on a Perkin-Elmer LS 55 luminescence spectrometer, equipped with a 20 kW xenon lamp.

2.2. Synthesis of compounds

$Zn_2(phen)(HPO_3)_2$ **1**: In a typical synthesis for **1**, a mixture of $Zn(AcO)_2 \cdot 2H_2O$ (0.220 g), H_3PO_3 (0.15 ml, 50 wt%), 1,10-phen (0.226 g) and ethylene glycol (3 ml) in a molar ratio of 1:1.1:1.4:54 was stirred under ambient conditions. The mixture was sealed in a Teflon-lined steel autoclave and heated at 160 °C for 2 days. The resulting product, consisting of colourless prism-like crystals, was recovered by filtration, washed with distilled water and alcohol, and finally dried at ambient temperature (86% yield based on zinc). The XRD pattern for the bulk product is in good agreement with the pattern based on single-crystal X-ray solution, indicating the phase purity (Fig. 1a). Elemental analysis showed that the sample contains 30.07, 2.05 and 5.62 wt% of C, H and N, respectively, in good accord with the expected values of 30.61, 2.14 and 5.95 wt% of C, H and N on the basis of the empirical formula given by the single-crystal structure analysis. IR(KBr, cm^{-1}) for **1**: 3416*s*, 3086*m*, 3067*m*, 2384*s*, 1624*m*, 1585*m*, 1519*s*, 1495*m*, 1428*s*, 1343*w*, 1222*w*, 1188*m*, 1154*m*, 1124*vs*, 1104*s*, 1069*m*, 1028*s*, 1003*s*, 870*m*, 853*s*, 782*w*, 724*s*, 648*m*, 574*m*, 562*s*, 452*m*, 426*m*.

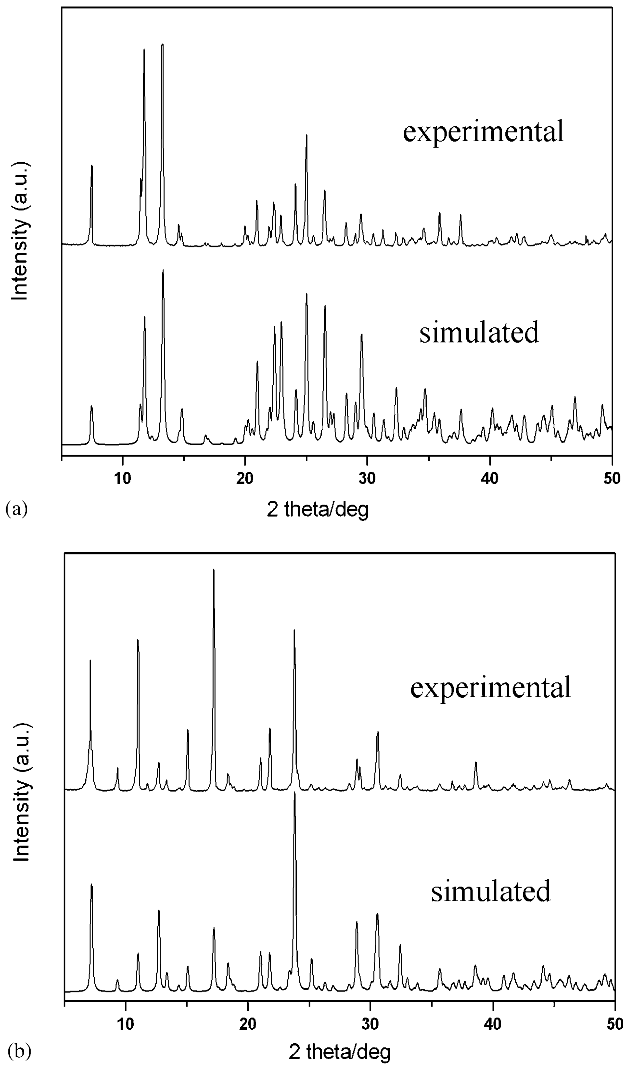

Fig. 1. Simulated and experimental power X-ray diffraction patterns of compounds **1** (a) and **2** (b).

$Zn(phen)(HPO_3)$ **2**: In a typical synthesis for **2**, a mixture of $Zn(AcO)_2 \cdot 2H_2O$ (0.347 g), H_3PO_3 (0.20 ml, 50 wt%), 1,10-phen (0.299 g) and ethanol (5 ml) in a molar ratio of 1:1:1.2:54 was stirred under ambient conditions. The resulting gel, was sealed in a Teflon-lined steel autoclave and heated at 130 °C for 3 days and then cooled to room temperature. Prism-like crystals were obtained which were recovered by filtration, washed with distilled water and dried in air (75% yield based on zinc). The XRD pattern for the bulk product is in good agreement with the pattern based on single crystal X-ray solution, proving the phase purity (Fig. 1b). Elemental analysis showed that the sample contains 44.01, 2.11 and 8.30 wt% of C, H and N, respectively, in good accord with the expected values of 44.27, 2.79 and 8.60 wt% of C, H and N on the basis of the empirical formula given by the single-crystal structure analysis. IR (KBr, cm^{-1}) for **2**: 3415*w*, 3092*w*, 3065*m*, 3046*m*, 3013*m*, 2347*s*, 1622*m*, 1590*m*, 1574*m*, 1513*s*, 1494*w*, 1449*w*, 1426*s*, 1345*m*, 1320*m*, 1227*m*, 1218*m*, 1141*vs*, 1102*s*, 1051*m*, 1032*m*, 1014*m*, 865*s*, 832*w*, 786*m*, 733*s*, 637*m*, 568*m*, 578*s*, 478*m*, 417*m*.

2.3. X-ray crystallography

Suitable single crystals of the as-synthesized compounds with dimensions of $0.10 \times 0.08 \times 0.06\,\mathrm{mm}^3$ for **1** and $0.40 \times 0.20 \times 0.10\,\mathrm{mm}^3$ for **2** were carefully selected under an optical microscope and glued to a thin glass fiber with epoxy resin. Crystal structure determination of **1** by XRD was performed on a Siemens SMART CCD diffractometer with graphite-monochromated Mo$K\alpha$ ($\lambda = 0.71073$ Å) radiation in the ω scanning mode at room temperature. An empirical absorption correction was applied using the SADABS program [12]. Crystal structure determination of **2** by XRD was performed on a Mercury-CCD diffractometer with graphite-monochromated Mo-$K\alpha$ ($\lambda = 0.71073$ Å) radiation in the ω scanning mode at room temperature. Empirical absorption corrections were applied using the CrystalClear program [13]. The structure of **1** was solved by the Patterson method and the structure of **2** was solved using direct methods, respectively. The zinc and phosphorus atoms were first located, and the carbon, nitrogen, and oxygen atoms were found in the final difference Fourier map. All the H atoms attached to the carbon were placed geometrically, and the remaining H atoms in the P–H groups in compounds **1** and **2** were located by Fourier maps. The structures were refined on F^2 by the full-matrix least-squares methods using the SHELX97 program package [14,15]. All non-hydrogen atoms were refined anisotropically. Experimental details for the structural determinations of **1** and **2** are presented in Table 1. Selected bond distances and angles for **1** and **2** are listed in Tables 2 and 3, respectively. CCDC reference numbers 259765 and 259766.

Table 1
Crystal data and structure refinement for compounds **1** and **2**

	1	**2**
Empirical formula	$C_{12}H_{10}N_2O_6P_2Zn_2$	$C_{12}H_9N_2O_3PZn$
Formula weight	470.90	325.55
Crystal system	Triclinic	Monoclinic
Space group	P-1	$C2/c$
a (Å)	8.1813(3)	16.1044(7)
b (Å)	8.5535(3)	18.9447(6)
c (Å)	12.3031(5)	8.1713(6)
α (deg)	75.609(1)	90
β (deg)	79.145(2)	94.175(4)
γ (deg)	67.157(2)	90
V (Å^3)	764.46(5)	2486.4(2)
Z	2	8
D_c (g cm^{-3})	2.046	1.739
μ (mm^{-1})	3.380	2.108
Reflns collected	3914	9482
Independent reflns	2622 [R (int) = 0.0379]	2851 [R (int) = 0.0242]
Final R indices [$I > 2\sigma(I)$]	$R_1 = 0.0682$, w$R_2 = 0.1505$	$R_1 = 0.0327$, w$R_2 = 0.0813$

$R_1 = \Sigma||F_o| - |F_{cs}||/\Sigma|F_o|$, w$R_2 = [\Sigma[w(F_o^2 - F_c^2)^2]/\Sigma[w(F_o^2)^2]]^{1/2}$.

3. Results and discussion

3.1. Synthesis and characterization

Compounds **1** and **2** were synthesized under solvothermal conditions. It can be found that the formations of compounds **1** and **2** are greatly influenced by the

Table 2
Selected bond lengths (Å) and angles (deg) for **1**[a]

Zn(1)–O(2)	1.910(7)	P(1)–O(1)	1.500(6)
Zn(1)–O(6)	1.925(6)	P(1)–O(3)	1.505(7)
Zn(1)–N(2)	2.054(7)	P(1)–O(2)	1.522(7)
Zn(1)–N(1)	2.068(7)	P(1)–H(1)	1.32(9)
Zn(2)–O(3)	1.908(7)	P(2)–O(5)	1.510(7)
Zn(2)–O(5)#1	1.918(6)	P(2)–O(4)	1.515(7)
Zn(2)–O(1)#2	1.939(6)	P(2)–O(6)	1.525(7)
Zn(2)–O(4)	1.953(7)	P(2)–H(2)	1.41(7)
O(2)–Zn(1)–O(6)	111.0(3)	O(1)–P(1)–O(3)	114.4(4)
O(2)–Zn(1)–N(2)	123.8(3)	O(1)–P(1)–O(2)	113.3(4)
O(6)–Zn(1)–N(2)	115.6(3)	O(3)–P(1)–O(2)	113.2(4)
O(2)–Zn(1)–N(1)	103.1(3)	O(1)–P(1)–H(1)	102(4)
O(6)–Zn(1)–N(1)	117.7(3)	O(3)–P(1)–H(1)	109(4)
N(2)–Zn(1)–N(1)	81.7(3)	O(2)–P(1)–H(1)	104(4)
O(3)–Zn(2)–O(5)#1	112.7(3)	O(5)–P(2)–O(4)	114.0(4)
O(3)–Zn(2)–O(1)#2	112.4(3)	O(5)–P(2)–O(6)	111.5(4)
O(5)#1–Zn(2)–O(1)#2	105.5(3)	O(4)–P(2)–O(6)	110.0(4)
O(3)–Zn(2)–O(4)	110.7(3)	O(5)–P(2)–H(2)	106(3)
O(5)#1–Zn(2)–O(4)	111.4(3)	O(4)–P(2)–H(2)	105(3)
O(1)#2–Zn(2)–O(4)	103.8(3)	O(6)–P(2)–H(2)	110(3)

[a] Symmetry transformations used to generate equivalent atoms: #1 $-x+1, -y+1, -z$; #2 $-x+1, -y+2, -z$.

Table 3
Selected bond lengths (Å) and angles (deg) for **2**[a]

Zn(1)–O(1)	2.004(2)	Zn(2)–O(3)#1	1.924(2)
Zn(1)–O(1)#1	2.004(2)	Zn(2)–O(2)#1	1.943(2)
Zn(1)–N(1)#1	2.174(2)	Zn(2)–O(2)	1.943(2)
Zn(1)–N(1)	2.174(2)	P(1)–O(3)#2	1.484(2)
Zn(1)–N(2)#1	2.302(2)	P(1)–O(1)	1.496(2)
Zn(1)–N(2)	2.302(2)	P(1)–O(2)	1.507(2)
Zn(2)–O(3)	1.924(2)	P(1)–H(1)	1.42(3)
O(1)–Zn(1)–O(1)#1	105.2(1)	N(2)#1–Zn(1)–N(2)	79.8(1)
O(1)–Zn(1)–N(1)#1	95.5(1)	O(3)–Zn(2)–O(3)#1	98.1(1)
O(1)#1–Zn(1)–N(1)#1	98.7(1)	O(3)–Zn(2)–O(2)#1	112.9(1)
O(1)–Zn(1)–N(1)	98.7(1)	O(3)#1–Zn(2)–O(2)#1	111.7(1)
O(1)#1–Zn(1)–N(1)	95.5(1)	O(3)–Zn(2)–O(2)	111.7(1)
N(1)#1–Zn(1)–N(1)	156.6(1)	O(3)#1–Zn(2)–O(2)	112.9(1)
O(1)–Zn(1)–N(2)#1	87.8(1)	O(2)#1–Zn(2)–O(2)	109.2(1)
O(1)#1–Zn(1)–N(2)#1	166.1(1)	O(3)#2–P(1)–O(1)	111.9(1)
N(1)#1–Zn(1)–N(2)#1	74.6(1)	O(3)#2–P(1)–O(2)	114.3(1)
N(1)–Zn(1)–N(2)#1	87.4(1)	O(1)–P(1)–O(2)	115.2(1)
O(1)–Zn(1)–N(2)	166.1(1)	O(3)#2–P(1)–H(1)	107.0(1)
O(1)#1–Zn(1)–N(2)	87.8(1)	O(1)–P(1)–H(1)	104.7(1)
N(1)#1–Zn(1)–N(2)	87.4(1)	O(2)–P(1)–H(1)	102.4(1)
N(1)–Zn(1)–N(2)	74.6(1)		

[a] Symmetry transformations used to generate equivalent atoms: #1 $-x+1, y, -z+1/2$; #2 $-x+1, -y, -z$.

zinc source and solvents. Using ZnO, $ZnCl_2$ or $ZnCO_3$ as zinc source, neither **1** nor **2** were obtained in similar experimental conditions. Using $Zn(OAc)_2 2H_2O$ as zinc source and ethylene glycol as solvent, the microcrystal of **1** was synthesized in the gels with molar ratios of 1 $Zn(AcO)_2 2H_2O$:1.1 H_3PO_3:1.4 phen:90 ethylene glycol. When decreasing the molar amount of ethylene glycol to 54 and keeping other conditions unchanged, the prism-like crystals of **1** was obtained, while increasing the molar amount of ethylene glycol more than 110, no crystals of **1** were prepared except for a thick gel. When the ethylene glycol as solvent was replaced by ethanol, compound **2** was synthesized. Later, by optimizing the reaction conditions, the yield of **2** reaches 75% based on zinc with 5 ml ethanol as solvent. However, if water (1, 2 or 3 ml) was added into the ethylene glycol or ethanol, neither **1** nor **2** were produced. If the solvent was replaced by glycerol, 1-butanol, pentaerythritol, 2-butanol or di(ethylene glycol), the amorphous phase or thick gel were produced. Therefore, the conclusion can be drawn that the category of solvents was critical for the growth of the crystals of **1** and **2**.

Thermogravimetric analysis of **1** and **2** were carried out under air atmosphere from 30 to 1200 °C with a heating rate of 15 °C min^{-1} (Fig. 2). The TG curve of **1** shows that it remains stable up to ~510 °C. The total weight loss of 35.91% observed between 510 and 1070 °C, corresponds to the removal of phen ligands, the dehydration of two HPO_3 groups (calcd 38.27% and 3.83% for one phen ligand and one H_2O molecule per formula unit, respectively), and the weight increase of 6.19% corresponding to aerial oxidation of P_2O_3 oxide (calcd ca. 6.8% from one P_2O_3 to one P_2O_5 molecule per formula unit). Assuming that the residue corresponds to ZnO and P_2O_5, the observed weight of the residue (64.1%) is in good agreement with the calculated value (64.7% for 2ZnO and P_2O_5 per formula unit). In addition, the residue is amorphous after the calcinations and its phase is unidentified.

For **2**, TG data show a broad weight loss of 53.27% over the range 300–950 °C assigned to the removal of phen ligands (calcd 55.36% for one phen molecule per formula unit), the dehydration (calcd 2.77% for 0.5 water molecule per formula unit, respectively) and the weight increase of 4.86% attributing to aerial oxidation of P_2O_3 oxide (calcd ca. 4.91% from $0.5P_2O_3$ to $0.5P_2O_5$ molecule per formula unit). Assuming that the residue corresponds to ZnO and P_2O_5, the observed weight of the residue (46.7%) is in good agreement with the calculated value (46.8% for ZnO and 0.5 P_2O_5 per formula unit). PXRD analysis indicates the residue for **2** is amorphous.

The photoluminescent spectra of **1**, **2** and phen were measured in the solid state at room temperature (Fig. 3). The emissive spectrum of **1** is composed of one strong band at 373 and one shoulder 384 nm ($\lambda_{ex} = 330$ nm), which may be assigned to ligand-to-metal charge transfer (LMCT). Upon excitation at 350 nm, **2** gives a strong emission band at $\lambda_{max} = 395$ nm, also assigned as LMCT. The slight red shift is aroused by the high coordination requirement between the Zn and phen ligands [17]. To the phen ligand, the emission is located at 361, 379 and 399 nm ($\lambda_{ex} = 340$ nm). The partial existence of the ligand-based emission in the fluorescence spectra of **1** and **2** suggests that the energy transfer from the ligand to the zinc centers is not effective and cannot sensitize the zinc emission to a large extent.

3.2. Structural description

The asymmetric unit of compound **1** contains 24 independent non-H atoms, including 2 zinc atoms, 2

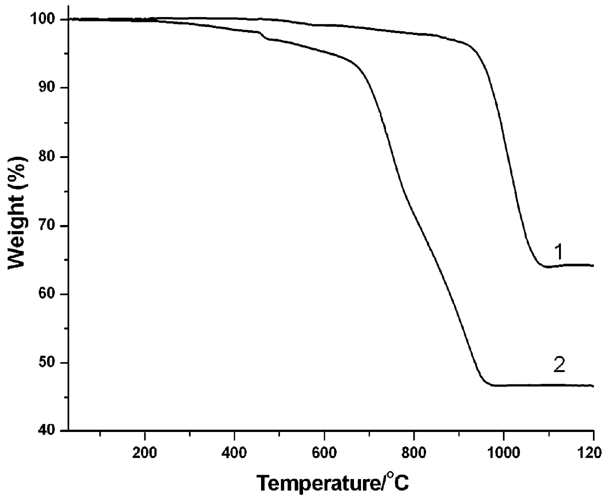

Fig. 2. The TG curve of **1** and **2** under air atmosphere (15 °C min^{-1}).

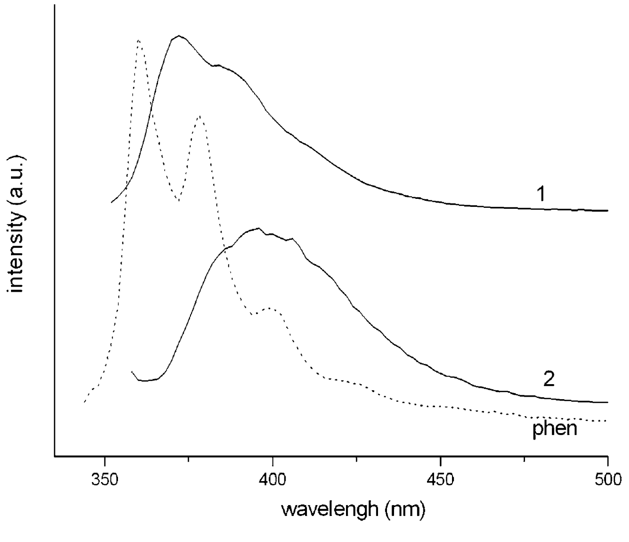

Fig. 3. The solid-state fluorescent spectrum of **1** ($\lambda_{ex} = 330$ nm), **2** ($\lambda_{ex} = 350$ nm) and phen ($\lambda_{ex} = 340$ nm) at room temperature.

phosphorus atoms, 6 oxygen atoms, 12 carbon atoms, and 2 nitrogen atoms, as shown in Fig. 4. Of the two unique tetrahedrally coordinated Zn atoms, Zn(1) atom is coordinated by 2 oxygen atoms and 2 nitrogen atoms from a phen ligand to form a ZnO_2N_2 tetrahedron. The Zn–O(N) bond lengths are in the range of 1.910(7)–2.068(7) Å. The Zn(2) is coordinated by 4 oxygen atoms, with Zn–O bond lengths in the range of 1.908(7)–1.953(7) Å. The phosphorus atoms each share 3 oxygen atoms with adjacent Zn atoms with P–O bond lengths ranging from 1.500(6) to 1.525(7) Å. The fourth tetrahedral vertex about each P atom is assumed to be a P–H bond [P1–H1 = 1.32(9) and P2–H2 = 1.41(7) Å]. The O–P–H and the O–P–O bond angles are in the range of 102(4)–114.4(4)°.

Compound **1** is a 1D chain-like structure containing 4-MR made of strictly alternating $Zn(2)O_4$ and HPO_3. The phen ligand coordinate Zn(1) atom to form a $[Zn(phen)]^{2+}$ complex that further link adjacent 2 HPO_3 groups from the chain to decorate the chain through two Zn–O–P bonds (Fig. 5). The adjacent chains are connected with each other through strong $\pi-\pi$ interactions of the phen ligands that are grafted onto the chains, as reflected in close (≈3.5 Å) intermolecular contacts.

The asymmetric unit of compound **2** contains 20 unique non-H atoms (2 Zn, 1 P, 3 O, 12 C, and 2 N) as shown in Fig. 6. All atoms, except Zn(1) and Zn(2) located on 2-fold symmetry, occupy general positions. The Zn(1) atom is coordinated by 2 oxygen atoms and 4 nitrogen atoms from 2 phen ligands to form an octahedron geometry. The Zn–O(N) bond distances are in the range of 2.004(2)–2.302(2) Å, with an average value of 2.160 Å. The tetrahedral Zn(2) atom shares 4 oxygen atoms with adjacent P atoms with Zn–O bond lengths in the range of 1.924(2)–1.943(2) Å. The P(1) atom links to 3 Zn atoms via bridging O atoms with P–O bond lengths ranging from 1.484(2) to 1.507(2) Å, and to a proton with the P–H = 1.42(3) Å, completing a pseudo-pyramid coordination characteristic of phosphorus (III). The O–P–H and the O–P–O bond angles are in the range of 102.4(1)–115.2(1)°.

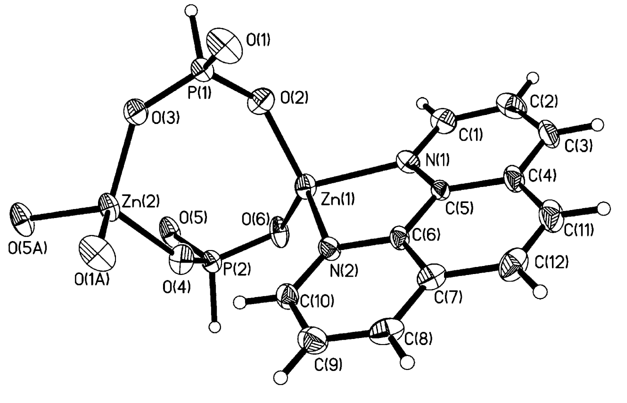

Fig. 4. ORTEP drawing of the asymmetric unit of **1** (50% thermal ellipsoids).

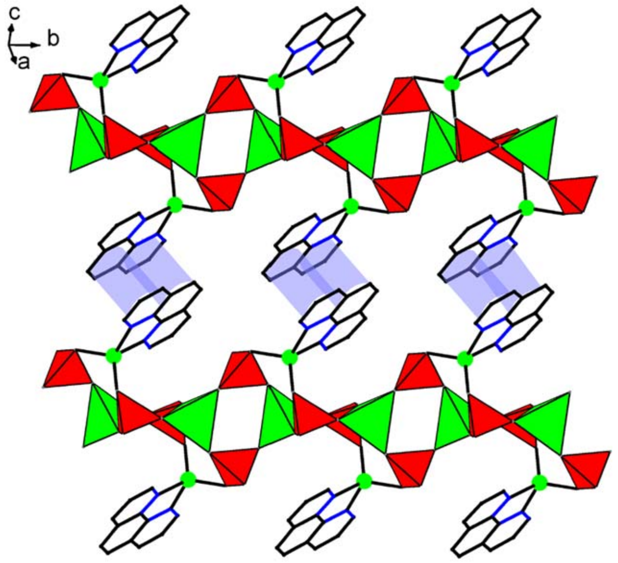

Fig. 5. View of the chain-like structure of **1**. ZnO_4, green, HPO_3, red. The face-to-face $\pi-\pi$ interaction is indicated by the purple column. Colour code: C, black; N, blue, Zn, green.

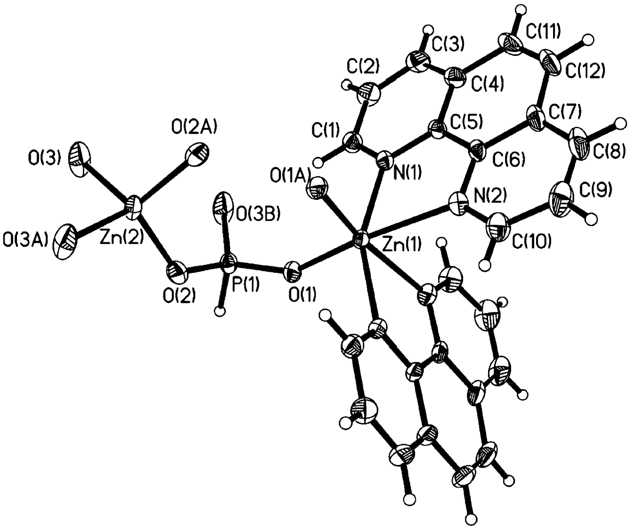

Fig. 6. ORTEP drawing of the asymmetric unit of **2** (50% thermal ellipsoids).

The structure of **2** is also a 1D chain that is the same as the structure of **1**. Two phen ligands coordinate Zn(1) atom to form a $[Zn(phen)_2]^{2+}$ complex that further decorates the chain. The adjacent chains are connected with each other through strong $\pi-\pi$ interactions of the phen ligands that are grafted onto the chains, which are interacted with 4 neighboring chains, as reflected in close (≈3.5 Å) intermolecular contacts (Fig. 7).

Analysis of the structures of **1** and **2** reveals a close relationship between them. Both of them are constructed from two distinct motifs, 1D chain and Zn-centered complex. As shown in Fig. 8a, the chains in **1** and **2** are same and consist of corner-shared 4-MRs made of ZnO_4 tetrahedra and HPO_3 pseudo-pyramids through sharing vertices. The different Zn-centered complexes, [ZnO_2(phen)] for **1** and [$ZnO_2(phen)_2$] for **2** (Fig. 8b,c), are linked to the chain via the Zn–O–P linkages, respectively, forming the chains of **1** and **2** (Figs. 8d,e).

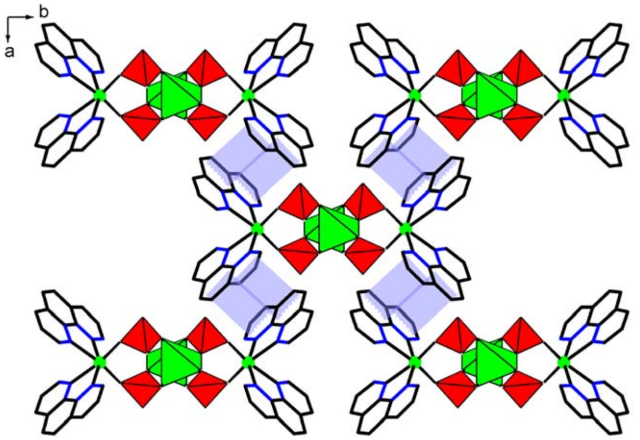

Fig. 7. Polyhedral view of the structure of **2** along the [001] direction. ZnO_4, green; HPO_3, red. The face-to-face $\pi-\pi$ interaction is indicated by the purple column. Colour code: C, black; N, blue, Zn, green.

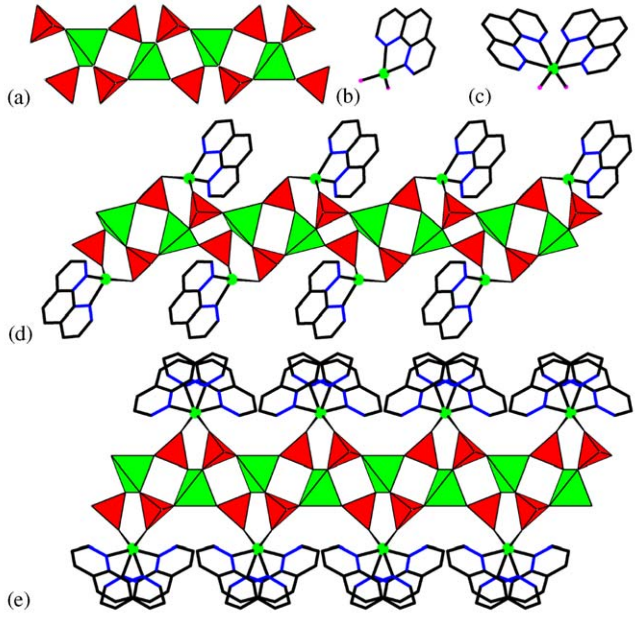

Fig. 8. (a) Polyhedral view of the linear chain constructed from ZnO_4 tetrahedra and HPO_3 pseudo-pyramid; (b) and (c) the second building blocks: ZnO_2(phen) and $ZnO_2(phen)_2$; (d) and (e) view of the structure of **1** along [010] direction and **2** along [0 0 1] direction. All H atoms attached to the C are omitted for clarity.

It is noteworthy that the two 1D chains of **1** and **2** are neutral and do not contain extra-framework cationic amines. As chain-like $(C_4N_3OH_7)_2 \cdot ZnHPO_3 \cdot H_2O$ [6a], the structural features of **1** and **2** are quite different from other chain-like metal phosphites observed previously, most of which contain cationic amines as charge-balancing agents and/or space fillers in their structures [8b,16].

4. Conclusions

In summary, this work describes the syntheses, structures and some properties of two new inorganic–organic hybrid zinc phosphites with neutral frameworks. Both are 1D chains made of corner-shared 4-MRs and decorated by Zn-centered complex architectures, $[Zn(phen)]^{2+}$ for **1** and $[Zn(phen)_2]^{2+}$ for **2**. These zinc phosphite chains are stably stacked into 2D and 3D supramolecular arrays for **1** and **2** via strong $\pi-\pi$ interactions. They are the first examples in the zinc-phosphite–phen system. Further investigation of metal phosphite prepared in presence of different rigid organic amine is in progress.

Acknowledgments

This work was supported by the NNSF of China (Grant Nos. 20271050 and 20473093), the Talents Program of the Chinese Academy of Sciences, and the NSF of Fujian Province (Grant Nos. E0510030 and E0210029).

References

[1] M.E. Davis, R.F. Lobo, Chem. Mater. 4 (1992) 756.
[2] P.B. Venuto, Microporous Mater. 2 (1994) 297.
[3] A.K. Cheetham, G. Férey, T. Loiseau, Angew. Chem. Int. Ed. 38 (1999) 3268.
[4] S.T. Wilson, B.M. Lok, C.A. Messina, T.R. Cannan, E.M. Flanigen, J. Am. Chem. Soc. 104 (1982) 1146.
[5] (a) J. Yu, R. Xu, Acc. Chem. Res. 36 (2003) 481;
(b) C.N.R. Rao, S. Natarajan, A. Choudhury, S. Neeraj, A.A. Ayi, Acc. Chem. Res. 34 (2001) 80.
[6] (a) W.T.A. Harrison, R.M. Yeates, M.L.F. Phillips, T.M. Nenoff, Inorg. Chem. 42 (2003) 1493;
(b) Z.-E. Lin, J. Zhang, S.-T. Zheng, Y.-W. Yao, G.-Y. Yang, Solid State Sci. 5 (2003) 1435.
[7] (a) N. Li, S. Xiang, J. Mater. Chem. 12 (2002) 1397;
(b) J.A. Rodger, W.T.A. Harrison, Chem. Commun. (2000) 2385;
(c) L.E. Gordon, W.T.A. Harrison, Inorg. Chem. 43 (2004) 1808.
[8] (a) S. Fernandez, J.L. Mesa, J.L. Pizarro, L. Lezama, M.I. Arriortua, R. Olazcuaga, T. Rojo, Chem. Mater. 12 (2000) 2092;
(b) W.T.A. Harrison, Int. J. Inorg. Mater. 3 (2001) 187;
(c) Y. Wang, J. Yu, Y. Li, Y. Du, R. Xu, L. Ye, J. Solid State Chem. 170 (2003) 303;
(d) Y. Wang, J. Yu, D. Yu, Z. Shi, Y. Zou, R. Xu, J. Chem. Soc., Dalton Trans. (2002) 4060;

(e) M.L.F. Phillips, T.M. Nenoff, C.T. Thompson, W.T.A. Harrison, J. Solid State Chem. 167 (2002) 337;
(f) W. Fu, Z. Shi, D. Zhang, G. Li, Z. Dai, X. Chen, S. Feng, J. Solid State Chem. 174 (2003) 11;
(g) Z.-E. Lin, J. Zhang, S.-T. Zheng, Y.-W. Yao, G.-Y. Yang, Solid State Sci. 6 (2004) 371.

[9] (a) Z. Shi, G. Li, D. Zhang, J. Hua, S. Feng, Inorg. Chem. 42 (2003) 2357;
(b) W. Fu, L. Wang, Z. Shi, G. Li, X. Chen, Z. Dai, L. Yang, S. Feng, Cryst. Growth Des. 2 (2004) 297;
(c) W.T.A. Harrison, M.L.F. Phillips, T.M. Nenoff, J. Chem. Soc. Dalton Trans. (2001) 2459;
(d) W.T.A. Harrison, J. Solid State Chem. 160 (2001) 4;
(e) W.T.A. Harrison, M.L.F. Phillips, T.M. Nenoff, Int. J. Inorg. Mater. 3 (2001) 1033;
(f) L. Wang, Z. Shi, W. Fu, G. Li, D. Zhang, W. Dong, Z. Dai, X. Chen, S. Feng, J. Solid State Chem. 177 (2003) 80;
(g) D. Zhang, Z. Shi, W. Dong, W. Fu, L. Wang, G. Li, S. Feng, J. Solid State Chem. 177 (2003) 343;
(h) W. Dong, G. Li, Z. Shi, W. Fu, D. Zhang, X. Chen, Z. Dai, L. Wang, S. Feng, Inorg. Chem. Commun. 7 (2003) 776;
(i) W. Fu, Z. Shi, G. Li, D. Zhang, W. Dong, X. Chen, S. Feng, Solid State Sci. 6 (2004) 225;
(j) Z.-E. Lin, J. Zhang, S.-T. Zheng, G.-Y. Yang, Microporous Mesoporous Mater. 68 (2004) 65;
(k) Z.-E. Lin, J. Zhang, S.-T. Zheng, G.-Y. Yang, J. Mater. Chem. 14 (2004) 1652;
(l) Z.-E. Lin, J. Zhang, S.-T. Zheng, G.-Y. Yang, Eur. J. Inorg. Chem. 5 (2004) 953.

[10] (a) W.T.A. Harrison, M.L.F. Phillips, J. Stanchfield, T.M. Nenoff, Inorg. Chem. 40 (2001) 895;
(b) J. Liang, Y. Wang, J. Yu, Y. Li, R. Xu, Chem. Commun. (2003) 882;
(c) J.-X. Pan, S.-T. Zheng, G.-Y. Yang, Microporous Mesoporous Mater. 75 (2004) 129.

[11] (a) Z.-E. Lin, J. Zhang, S.-T. Zheng, G.-Y. Yang, Inorg. Chem. Commun. 6 (2003) 1035;
(b) Z.-E. Lin, Y.-W. Yao, J. Zhang, G.-Y. Yang, J. Chem. Soc., Dalton Trans. (2003) 3160;
(c) Z.-E. Lin, Y.-Q. Sun, J. Zhang, Q.-H. Wei, G.-Y. Yang, J. Mater. Chem. 13 (2003) 447.

[12] G.M. Sheldrick, A program for the Siemens Area Detector ABSorption correction, University of Göttingen, 1997.

[13] Rigaku Corp. CrystalClear 1.3.6, Software User's Guide for the Rigaku R-AXIS and Mercury and Jupiter CCD Automated X-ray Imaging System, Molecular Structure Corporation, 2000.

[14] G.M. Sheldrick, SHELXS97 Program for Solution of Crystal Structures, University of Göttingen, Germany, 1997.

[15] G.M. Sheldrick, SHELXL97 Program for Solution of Crystal Structures, University of Göttingen, Germany, 1997.

[16] A. Kirkpatrick, W.T.A. Harrison, Solid State Sci. 6 (2004) 593.

[17] T. Gunnlaugsson, J.P. Leonard, K. Sénéchal, A.J. Harte, Chem. Commun. (2004) 782.